Comparative study of one-dimensional photonic crystal heterostructure doped with a high and low-transition temperature superconducting for a low-temperature sensor

A. Soltani[a], F. Ouerghi[a], F. AbdelMalek[a], S. Haxha[b]

[a]*Advanced Materials and Quantum Phenomena Laboratory, Physics Department, Faculty of Sciences, University of Tunis-El Manar, 2092, Tunisia*

[b]*Department of Electronic Engineering School of Engineering, Physical and Mathematical Sciences Royal Holloway, University of London, Egham, Surrey, TW20 0EX, United Kingdom*

Abstract: In this work, we present a theoretical study dealing with the sensitivity to physical parameters such as defect nature and thickness, and temperature. Indeed, the sensitivity considerably enhanced via the use of one-dimensional photonic crystal heterostructure (1D-PCH) which is composed of a few layers of ordinary materials, and superconducting defects. The aim of this paper is to compare the sensitivity of two proposed models consisting of (a) 1D-PCH doped with a high-transition temperature superconductor (Yttrium barium copper oxide (YBCO)), and (b) 1D-PCH doped with a low-transition temperature superconductor (niobium nitrure (NbN)). By using the transfer-matrix method (TMM), it has been demonstrated that model (b) is very sensitive compared to model (a). Therefore, the superconducting defect nature on 1D-PCH, using a few layers can play a fundamental role in a very low-temperature sensor.

1. Introduction

A photonic crystal (PC) is an assemblage of alternating dielectric materials whose refractive index varies periodically in one, two or three directions of the space. This periodicity makes it possible to create a photonic band gap (PBG) [1–3]. The development of this new type of new materials at PBG opens new perspectives for the study of promising applications used in the field of optoelectronics. The technological progress in the nanometer-manufacturing field facilitates the manufacture of sophisticated devices produced from PCs such as PC waveguides [4,5], the PC filter [6,7], and lately the PC optical diode [8,9]. The tunable-filter application, which has recently widely been used, is based on several kinds of materials like liquid crystals [10], semiconductors [11], and magnetic fluids [12]. 1D-PC structures have been proposed over the last past years, and been subject to intense research because this class of the PCs is the simplest to manufacture. The width and the spectral position of the PBG depend on the material parameters which are refractive indices and the thickness of the alternate materials [13,14]. By introducing a variety of nonconventional materials, we can modulate the capability of the PC. In fact, dielectric-superconducting photonic crystals are suitable to achieve a tunable-filter and a low-temperature sensor. This is due to the special electromagnetic properties of these superconducting materials whose permittivity is widely dependent on the temperature, and the external field [10–18].

Recently, several research works have tackled the study of unidimensional and bi-dimensional superconducting PCs [19–21]. These works aim at the low-temperature sensor application through the variation of the temperature and the geometry of device. For example, Srivastava has analyzed the position of the transmission mode by varying the thicknesses of the superconducting defects (high and lowtransition temperature superconductors) in 1D-PC [16]. However, he has found a low PBG having around 450 nm, and not totally stable. Ji-Jiang Wu et al. have also analyzed the position of the transmission mode via varying the temperature, using 1D-PCH containing a hightransition temperature superconductor. However, they have used a significant number of layers, and found a low value of the average change (7.313 nm/K), and that the PBG is not as broad, which limits its fields of application [17]. Furthermore, Z. Baraket et al. have analysed the optical response of a ternary dielectric superconductor photonic crystal undergoing a symmetrical linear deformation of thickness of each layer. They have used the average change of the transmission mode, reaching 42.2 nm [18], but the quantity of materials and the simplicity of experience still remain a challenge. The purpose of this work is to overcome such problems. We propose a short binary 1D-PCH containing a superconducting defect layer designed as (HL)N D (LH)N. The results show different behaviors in terms of sensitivity for 1D-PCH doped with YBCO (model (a)), and then doped with NbN (model (b)) in the visible region. Therefore, the effect of the nature and thicknesses of superconducting defect layers and the impact of temperature on the displacement of transmission modes could be analyzed.

2. Theoretical model

In this study, we have used the TMM to calculate the transmission spectra [22–24]. In our calculation, a transverse-magnetic wave is considered, i.e. the electric field is parallel to the y–z plan of layers. During the calculation, both effects such as thermal-expansion and thermal–optical are taken into account. The thickness d(T) and the refractive index of the medium n(T) can be changed because of those effects. The thickness and refractive index are given as follows;

$$d(T) = d_0(1 + \alpha \Delta T) \quad (1)$$

$$n(T) = n_0(1 + \beta \Delta T) \quad (2)$$

where α is the thermal-expansion effect coefficient, and ΔT is the temperature deviation. What is more, $d0$ is the thickness of the layer at a room temperature. β is also the thermo-optic coefficient, and $n0$ is the refractive index of the layer at a room temperature. The electromagnetic response of the superconducting material can be well described by the two-fluid models, together with the London local electrodynamics. Hence, for the superconducting material, the refractive index is described by the Gorter–Casmir two-fluid models [25,26]. Here, we suppose that the superconducting material is non-magnetic (μs = 1). The complex conductivity of a superconducting is as reported in [27], and as follows;

$$\sigma = -\frac{i}{\omega \mu_0 \lambda_L^2} \quad (3)$$

where λL represents the temperature-dependent London penetration depth :

$$\lambda_L = \frac{\lambda_0}{[(1 - (T/T_c))^p]^{1/2}} \quad (4)$$

in which $\lambda 0$ is the London-penetration depth at T = 0 K, and Tc is the transition temperature of the superconductor. Moreover, the exponent p takes the value 2 for a high-transition temperature superconductor (Tc>77 K), and the value 4 for a low-transition temperature superconductor (Tc<77 K) [16]. Thus, the dielectric function of the superconductor can be written as:

$$\varepsilon_s(\omega, T) = 1 - \left(\frac{1}{\omega \mu_0 \varepsilon_0 \lambda_L^2}\right) \quad (5)$$

where ω, $\varepsilon 0$ and $\mu 0$ are the frequency, the permittivity and permeability of vacuum, respectively. It can be clearly seen that the permittivity of the superconducting material is sensitive to the wavelength and temperature. When we vary the structure temperature, the refractive index and/or the thickness of each layer may be changed according to Eqs. (1), (2) and (5). Consequently, the average change of the transmission mode might be changed, too. This average change can be expressed as the sensitivity of the structure [28,29].

3. Numerical results and discussion

In this work, we have selected the low-temperature sensor obtained by 1D-PCH doped by a superconducting-defect layer. The tenability of the sensor highly depends on the nature and the thicknesses of the superconducting-defect layers, and mostly on the temperature. Consequently, Fig. 1 represents our short binary structure marked as (HL)ND (LH)N, where H, L and D layers identify Si, SiO2 and superconducting defect layer (YBCO or NbN), respectively. The number of periods N equals 3. The dielectric layers have refractive indices, which are nSi =3.45 and $nSiO2$ = 1.45, at room temperature. The thickness dSi and $dSiO2$ of the dielectric layers are taken according to the quarter wave stack condition given as $nSidSi = nSiO2dSiO2 = \lambda c\ 4$, where λc is the central wavelength assumed to be 830 nm and around the first window of telecom.

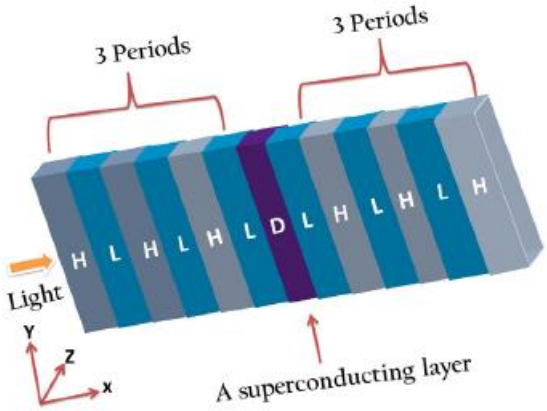

Fig. 1. Schematic representation of a short binary 1D-PCH doped with superconducting defect layer.

In the following calculations, the thermal-expansion coefficients of Si and SiO2 are 2.6×10−6/K and 0.55×10−6/K, respectively. The thermo-optic coefficients of the same dielectrics (Si and SiO2) are 166×10−6/K and 1×10−5/K, respectively [30,31]. We hereafter closely search the impact of the superconducting defect layers on the spectral properties of the transmission mode. The subsequent parameter of the YBCO marked by the thermal-expansion coefficient is equal to 13.35×10−6/K. Furthermore, the transition temperature of YBCO defect is Tc= 92 K, and its London-penetration depth is $\lambda 0(Y\ BCO)$= 140 nm at zero temperature [32]. The optical parameters of the NbN defect are considered as a thermal-expansion coefficient equal to 10.1×10−6/K, the transition temperature equals 16 K, and the London-penetration depth is $\lambda 0(NbN)$= 200 nm at zero temperature [33]. The comparative study dealing with the sensitivity of transmission mode to the physical parameters of the two models has been analysed in the following three parts. The first part deals with the comparative study of two models in terms of dispersion and tenability of the transmission mode according to the nature of the superconducting defect. In this part, we have chosen a temperature value below the transition temperature of the two superconducting defects (T = 15.8 K), and a superconducting defect thickness equal to 50 nm. The transmission spectra of three structures at various superconducting defects are shown in Fig. 2. The black curve set out the transmission spectrum of 1D-PCH without a superconducting defect; the red curve shows the transmission spectrum of model (a); and the green curve introduces the transmission spectrum of model (b).

We have noticed in this figure that the PBG interval has approximately been placed in 640 nm–1320 nm, so the PBG value equals more than 680 nm. It is clear the width of the PBG has no visible difference for all the three curves. On the other hand, the transmission mode moves according to the defect nature. First, the black curve shows that the selective transmission mode is centered around 842 nm, and this mode is of zero dispersion because its transmission amplitude equals 1. Second, as the permittivity of superconducting materials can be tuned by the system temperature and the external magnetic field, the red curve indicates a transmission mode shifted towards

the higher wavelengths compared to the black curve. This mode is centred in 846 nm, so the shift equals 4 nm and is followed by a decrease to 0.97 in the transmission amplitude. Third, for the green curve, it is obvious that the transmission mode has been shifted from 842 nm to λ = 880 nm (the shift equals 38 nm), and the transmission

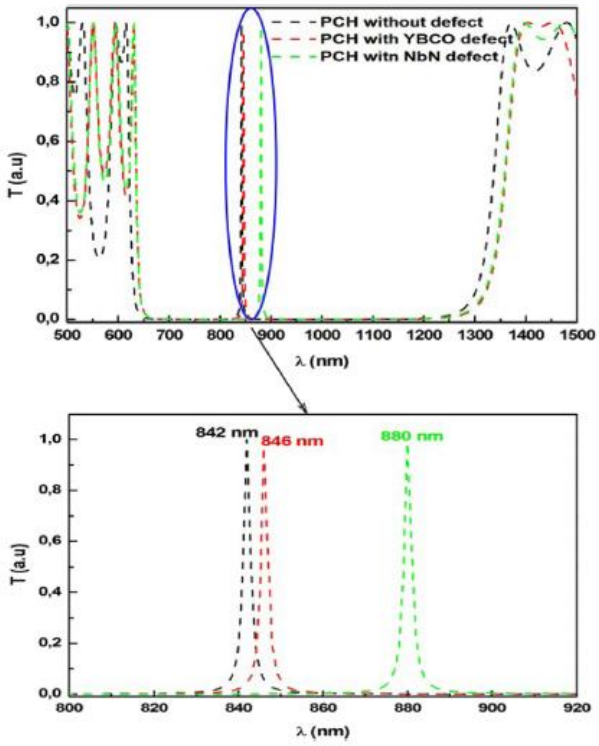

amplitude in this case equals 0.99. We assess, at a lower temperature (<16 K), the transmission mode of model (b) has been shifted 9.5 times, compared to model (a), towards the higher wavelengths. Therefore, the nature of superconducting material has a tremendous impact on the position of the transmission mode with minimum of dispersion because this family of materials is highly sensitive to any variation in the temperature and external field.

Fig. 2. Transmission of 1D-PCH without defect (black curve), with YBCO defect (red curve) and with NbN defect (green curve), at T = 15.8 K for ds = 50 nm . (For interpretation of the references to color in this figure legend, the reader is referred to the web version of this article.)

This second part aims to compare the variation of the transmission mode for the two models at various thicknesses of superconducting defect layers. Fig. 3 shows a 3D plot of the transmission mode of two models for various thicknesses of the superconducting defect as the temperature is fixed at 15.8 K. It is clear in Fig. 3(a) the transmission mode can be tuned when the thickness of the YBCO increases from 10 nm to 50 nm, with a step of 10 nm. More precisely, it is remarkable in this figure that the transmission mode is localized in 843 nm for ds = 10 nm, and in 844 nm for ds = 20 nm. Moreover, for ds = 30 nm, the peak position is at 845 nm while it is centered at 846 nm when ds = 40 nm, and for ds = 50 nm, the peak is localized at 847 nm. The displacement of this mode is about 4 nm in [10–50] nm thickness range. This undesired shift towards the highest wavelengths above spurs us on to try another type of a superconducting defect. Hence, we investigate the impact of the variation of NbN thickness in the same range. As shown in Fig. 3(b), the transmission mode is undergoing an important shift. The shift is about 30 nm because for ds= 10 nm (black curve), the peak is localized in 850 nm, and moves to 880 nm for ds = 50 nm (sky blue curve). We have found that the transmission mode is distant from each other, approximately by 7 nm. As a result, the transmission mode can strongly be tuned to the long wavelengths through the increasing NbN thickness. In order to confirm the ultra-sensitivity of model (b), we have ended this part by calculating the quality factor (Q) for the two models at the same temperature of 15.8 K, and at the same thickness (ds = 50 nm). We notice in Fig. 3, the full width at half maximum (FWHM) of the transmission modes slightly increases. Q is proportional to FWHM since it could be written as:

$$Q = \frac{\lambda_p}{\Delta\lambda} \quad (6)$$

where λp is the resonance wavelength of the superconducting defect layer, and $\Delta\lambda$ is the FWHM. Consequently, the numerical computation has shown the Q of model (b) equals 440 and the Q of model (a) equals 423.5. Eventually, the transmission mode of model (b) has been shifted 7.5 times compared to model (a), and the quality factor of model (b) is the most important in model (a). Thus, model (b) is a satisfying device in designing a very low-temperature sensor.

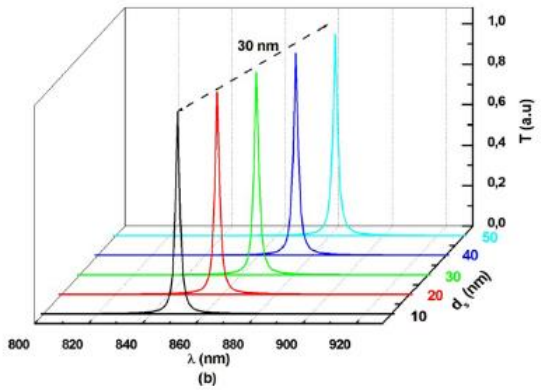

Fig. 3. Variation of the transmission mode of (a) 1D-PCH with different YBCO layer thickness and (b) 1D-PCH with different NbN layer thickness at T = 15.8 K . (For interpretation of the references to color in this figure legend, the reader is referred to the web version of this article.)

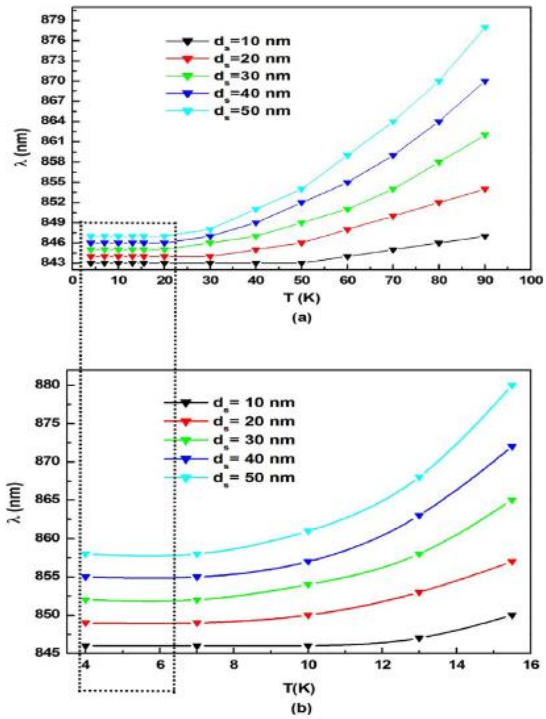

Fig. 4. The variation of the transmission mode for different temperature values and for various superconducting thicknesses dS of 1D-PCH (a) with the YBCO defect and (b) with the NbN defect.

This third part aims at tackling the comparative study in the variation of the transmission mode with temperature for the two models at different superconducting defect thickness. It can be seen in Fig. 4 that the temperature sensitivity has improved when the thickness of the defect layer ds increases in the [10–50] nm range. The calculation of the transmission mode variation in [4-90] K temperature range for the model (a) reported in Fig. 4(a). The dashed zone in this figure showing the transmission response of the structure designed is not sensitive in [4-40] K temperature range. However, it rapidly increases with a temperature above 40 K. The most remarkable effect is assumed at ds = 50 nm because the transmission mode is observed in a non-linear relation with the temperature. This thickness of the superconducting may be an important parameter having the ability to improve the performance of the devices since it generates possible shifts of the transmission mode. As a consequence, for ds = 50 nm, the transmission mode is very sensitive to the temperature, and the average change in this mode equals 31 nm/K in [4-90] K temperature range. Hence, we have to get the important average with a short binary 1D-PCH. On the other hand, the calculations of the transmission mode variation for model (b) to temperature are also performed. In Fig. 4(b), the dashed zone shows the linearly-transmission mode variation that does not go beyond 7 K temperature in this case. When we exceed this temperature, the transmission mode variation is non-linear. It is obvious that, for a thickness ds = 50 nm and in [4 −15.8] K temperature range, the average change equals 22 nm/K. It is a satisfying value for a very low range of temperature. We have noted that model (b) presents a high enhancement of the sensitivity in the range of temperature below 16 K. Thus, the analysis presented suggests an alternative that can be used to design a very low-temperature sensor.

4. Conclusion

In conclusion, we have investigated the sensitivity of 1D-PCH with a superconducting defect in accordance with physical parameters, using a few layers and the TMM method. It is worth noting that the shift of the transmission mode depends on the nature and thickness of the superconducting defect layer and the temperature. We have firstly examined the comparative study in terms of dispersion and the tenability under the nature of superconducting defect, when T = 15.8 K and ds = 50 nm. We have proved that the transmission mode of model (b) has shifted 9.5 times compared to model (a). We have secondly fixed T as 15.8 K, and we have varied the superconducting-defect thicknesses in [10–50] nm range. We have denoted that the transmission mode of model (b) has shifted 7.5 times compared to model (a), and this quality factor is very satisfying compared to model (a). Finally, for ds = 50 nm, the temperature variation has shown that the average change in model (b) is equal to 22 nm/K. Thus, the analysis presented suggests the few layers of 1D-PCH doped with NbN superconducting defect at higher sensitivity opens the prospect for the very low-temperature sensor application.

Acknowledgments

This work is main supported by the ‘‘Ministère de l’Enseignement Supérieur, de la Recherche Scientifique et de la Technologie’’ (LR11ES10) (Tunisia).

References

[1] J.G. Fleming, S.Y. Lin, Three-dimensional photonic crystal with a stop band from 1.35 to 1.95 m, Opt. Lett. 24 (1999) 49–51.

[2] F. Ouerghi, F. AbdelMalek, S. Haxha, E.K. Akowuah, H. Ademgil, Design of multicavities on left-handed photonic-crystal based chemical sensors, IEEE J. Lightw. Technol. 30 (2012) 3288–3293.

[3] F. Scotognella, Four-material one dimensional photonic crystals, Opt. Mater. 34 (2012) 1610–1613.

[4] L.H. Frandsen, Y. Elesin, L.F. Frellsen, M. Mitrovic, Y. Ding, O. Sigmund, K. Yvind, Topology optimized mode conversion in a photonic crystal waveguide fabricated in silicon-insulator material, Opt. Express 22 (2014) 8525–8532.

[5] E. Gunasundari, K. Senthilnathan, S. Sivabalan, Abdosllam M. Abobaker, K. Nakkeeran, P. Ramesh Babu, Waveguiding properties of a silicon nanowire embedded photonic crystal fiber, Opt. Mater. 36 (2014) 958–964.

[6] M. Zamani, Photonic crystal-based optical filters for operating in second and third optical fiber windows, Superlattices Microstruct. 92 (2016) 157–165.

[7] S. Sahel, R. Amri, L. Bouaziz, D. Gamra, M. Lejeune, M. Benlahsen, K. Zellama, H. Bouchriha, Optical filters using Cantor quasi-periodic one dimensional photonic crystal based on Si/SiO2, Superlattices Microstruct. 97 (2016) 429–438.

[8] A. Soltani, F. Ouerghi, F. AbdelMalek, S. Haxha, H. Ademgil, E.K. Akowuah, Unidirectional light propagation photonic crystal waveguide incorporating modified defects, Optik 130 (2017) 1370–1376.

[9] A. Soltani, F. Ouerghi, F. AbdelMalek, S. Haxha, H. Ademgil, E.K. Akowuah, Effect of the elliptic rods orientations on the asymmetric light transmission in photonic crystals, Opt. Commun. 392 (2017) 147–152.

[10] T. Yasuda, Y. Tsuji, M. Koshiba, Tunable light propagation in photonic crystal coupler filled with liquid crystal, IEEE photonics Technol. Lett. 17 (2005) 55–57. [11] T.C. King, Y.P. Yang, Y.S. Liou, C.J. Wu, Tunable defect mode in a semiconductor-dielectric photonic crystal containing extrinsic semiconductor defect, Solid State Commun. 152 (2012) 2189–2192.

[12] S.L. Pu, S.H. Dong, J. Huang, Tunable slow light based on magnetic-fluid infiltrated photonic crystal waveguides, J. Opt. 16 (2014) 045102.

[13] F. Wang, Y.Z. Cheng, X. Wang, D. Qi, H. Luo, R.Z. Gong, Effective modulation of the photonic band gap based on Ge/ZnS one-dimensional photonic crystal at the infrared band, Opt. Mater. 75 (2018) 373–378.

[14] S.M. Weiss, M. Haurylau, P.M. Fauchet, Tunable photonic bandgap structures for optical interconnects, Opt. Mater. 27 (2005) 740–744.

[15] C.A. Hu, J.W. Liu, C.J. Wu, T.J. Yang, S.L. Yang, Effects of superconducting film on the defect mode in dielectric photonic crystal heterostructure, Solid State Commun. 157 (2013) 54–57.

[16] S.K. Srivastava, Study of defect modes in 1d photonic crystal structure containing high and low Tc superconductor as a defect layer, J. Supercond. Nov. Magn. 27 (2014) 101–114.

[17] J.J. Wu, J.X. Gao, Temperature-dependent optical properties of defect mode in dielectric photonic crystal heterostructure containing a superconducting layer, Mater. Chem. Phys. 171 (2016) 91–96.

[18] Z. Baraket, J. Zaghdoudi, M. Kanzari, Investigation of the 1d symmetrical linear graded superconductor dielectric photonic crystals and its potential applications as an optimized low temperature sensors, Opt. Mater. 64 (2017) 147–151.

[19] Francis Segovia-Chavesa, Herbert Vinck-Posada, Thermo-optic effect on the photonic band structure in a two dimensional square lattice photonic crystal, Optik 180 (2019) 1–7.

[20] Zhang Hai-Feng, The Mie resonance and dispersion properties in the twodimensional superconductor photonic crystals with fractal structure, Physica C 550 (2018) 65–73.

[21] Charles-Edouard Bardyn, Michele Filippone, Thierry Giamarchi, Bulk pumping in two-dimensional topological phases, Phys. Rev. B 99 (2019) 035150.

[22] D. Qi, X. Wang, Y. Cheng, R. Gong, B. Li, Design and characterization of onedimensional photonic crystals based on ZnS/Ge for infrared-visible compatible stealth applications, Opt. Mater. 62 (2016) 52–56.

[23] Z.F. Sang, Z.Y. Li, Properties of defect modes in one-dimensional photonic crystals containing a graded defect layer, Opt. Commun. 273 (2017) 162–166.

[24] Hussein A. Elsayed, A multi-channel optical filter by means of one dimensional n doped semiconductor dielectric photonic crystals, Mater. Chem. Phys. 216 (2018) 191–196.

[25] A.H. Aly, S.W. Ryu, H.T. Hsu, C.J. Wu, THZ transmittance in one-dimensional superconducting nanomaterial-dielectric superlattice, Mater. Chem. Phys. 113 (2009) 382–384.

[26] M. Tinkham, Introduction To Superconductivity, McGraw-Hill, New York, 1996.

[27] C.A. Hu, J.W. Liu, C.J. Wu, T.J. Yang, S.L. Yang, Effects of superconducting film on the defect mode in dielectric photonic crystal heterostructure, Solid. State. Commun. 157 (2013) 54–57.

[28] E.K. Akowuah, T. Gorman, S. Haxha, Design and optimization of a novel surface plasmon resonance biosensor based on Otto configuration, Opt. Express 17 (2009) 23511–23521.

[29] A. Bouali, Shyqyri Haxha, Fathi AbdelMalek, M. Dridi, Habib Bouchriha, Tuning of plasmonic nanoparticle and surface enhanced wavelength shifting of a nanosystem sensing using 3-D-FDTD method, IEEE J. Quant. Electro. 50 (2014) 651–657.

[30] Y.H. Chang, Y.Y. Jhu, C.J. Wu, Temperature dependence of defect mode in a defective photonic crystal, Opt. Commun. 285 (2011) 1501–1504.

[31] Y.P. Varshni, Temperature dependence of the energy gap in semiconductors, Physica 34 (1967) 149–154.

[32] J. Kawashima, Y. Yamada, I. Hirabayashi, Critical thickness and effective thermal expansion coefficient of YBCO crystalline film, Physica C 306 (1998) 114–118.

[33] H. Holleck, Material selection for hard coatings, J. Vac. Sci. Technol. A 4 (1986) 2661–2669.